

Geological Society of America Special Papers Online First

Ground-motion site effects from multimethod shear-wave velocity characterization at 16 seismograph stations deployed for aftershocks of the August 2011 Mineral, Virginia, earthquake

William J. Stephenson, Jack K. Odum, Daniel E. McNamara, et al.

Geological Society of America Special Papers, published online September 30, 2014;
doi:10.1130/2015.2509(03)

E-mail alerting services click www.gsapubs.org/cgi/alerts to receive free e-mail alerts when new articles cite this article

Subscribe click www.gsapubs.org/subscriptions to subscribe to Geological Society of America Special Papers

Permission request click www.geosociety.org/pubs/copyrt.htm#gsa to contact GSA.

Copyright not claimed on content prepared wholly by U.S. government employees within scope of their employment. Individual scientists are hereby granted permission, without fees or further requests to GSA, to use a single figure, a single table, and/or a brief paragraph of text in subsequent works and to make unlimited copies of items in GSA's journals for noncommercial use in classrooms to further education and science. This file may not be posted to any Web site, but authors may post the abstracts only of their articles on their own or their organization's Web site providing the posting includes a reference to the article's full citation. GSA provides this and other forums for the presentation of diverse opinions and positions by scientists worldwide, regardless of their race, citizenship, gender, religion, or political viewpoint. Opinions presented in this publication do not reflect official positions of the Society.

Notes

The Geological Society of America
Special Paper 509
2015

Ground-motion site effects from multimethod shear-wave velocity characterization at 16 seismograph stations deployed for aftershocks of the August 2011 Mineral, Virginia, earthquake

William J. Stephenson
Jack K. Odum
Daniel E. McNamara
Robert A. Williams
Stephen J. Angster

U.S. Geological Survey, Box 25046, MS 966, Denver, Colorado 80225, USA

ABSTRACT

We characterize shear-wave velocity versus depth (V_s profile) at 16 portable seismograph sites through the epicentral region of the 2011 M_w 5.8 Mineral (Virginia, USA) earthquake to investigate ground-motion site effects in the area. We used a multimethod acquisition and analysis approach, where active-source horizontal shear (SH) wave reflection and refraction as well as active-source multichannel analysis of surface waves (MASW) and passive-source refraction microtremor (ReMi) Rayleigh wave dispersion were interpreted separately. The time-averaged shear-wave velocity to a depth of 30 m (V_{s30}), interpreted bedrock depth, and site resonant frequency were estimated from the best-fit V_s profile of each method at each location for analysis. Using the median V_{s30} value (270–715 m/s) as representative of a given site, we estimate that all 16 sites are National Earthquake Hazards Reduction Program (NEHRP) site class C or D. Based on a comparison of simplified mapped surface geology to median V_{s30} at our sites, we do not see clear evidence for using surface geologic units as a proxy for V_{s30} in the epicentral region, although this may primarily be because the units are similar in age (Paleozoic) and may have similar bulk seismic properties. We compare resonant frequencies calculated from ambient noise horizontal:vertical spectral ratios (HVSr) at available sites to predicted site frequencies (generally between 1.9 and 7.6 Hz) derived from the median bedrock depth and average V_s to bedrock. Robust linear regression of HVSr to both site frequency and V_{s30} demonstrate moderate correlation to each, and thus both appear to be generally representative of site response in this region. Based on Kendall tau rank correlation testing, we find that V_{s30} and the site frequency calculated from average V_s to median interpreted bedrock depth can both be considered reliable predictors of weak-motion site effects in the epicentral region.

INTRODUCTION

Moderate earthquakes in the eastern United States are rare, but their societal impact can be extensive (Horton and Williams, 2012). The 2011 M_w 5.8 Mineral (Virginia, USA) earthquake highlighted important regional ground effects that contributed to this impact, including a northeast-trending expanded felt region (as observed in U.S. Geological Survey “Did You Feel It?” website responses; <http://earthquake.usgs.gov/earthquakes/dyfi/>), anisotropic wave propagation patterns along prevailing tectonic fabric (McNamara et al., 2014a), low ground-motion attenuation (e.g., McNamara et al., 2014b), and extensive wide-ranging rock-falls at distances to three times as great as would be predicted from western U.S. earthquake observations (Jibson and Harp, 2012).

Hough (2012) ascribed differences in the U.S. Geological Survey website “Did You Feel It?” intensity units and peak ground accelerations of as much as 1.5 and 3, respectively, to variability in site response. As governed by localized geology and site soil properties, site response can be a major contributor to observed ground motion and to variations in ground shaking intensity (Aki, 1988; Borchardt and Glassmoyer, 1992; Harmsen, 1997). Shear-wave velocity (V_s) of the shallow geologic column is a key geophysical parameter used for assessing site response in seismic ground-motion investigations because of its impact on near-surface wavefield propagation (e.g., Borchardt, 1970; Joyner et al., 1981; Cramer et al., 2004; Boore, 2004; Frankel et al., 2009).

The time-averaged shear-wave velocity to a depth of 30 m (V_{s30}) is used extensively in building design codes (e.g., International Code Council, 2006), earthquake-engineering applications (Borchardt, 1994; Kramer, 1996; Boore et al., 1997; Wills and Silva, 1998; Dobry et al., 2000), and ground-motion prediction-equation relationships (Zhao and Xu, 2013). Proxies for V_{s30} , including surface geology-, slope-, and terrain-based methods have been developed to predict V_{s30} where direct measurements are sparse (Wills et al., 2000; Wald and Allen, 2007; Yong et al., 2012). However, these methods are not always reliable, prompting both Thompson and Wald (2012) and Yong et al. (2012) to suggest that expansion of ground-truth V_s measurement databases is a key component for improving the predictive capabilities of proxy methods. V_s site characterization data in regions not commonly exposed to earthquakes are very limited. The 2011 Mineral earthquake has offered a unique opportunity to expand the number of V_s observations in a region that has few large earthquakes.

Site response can be broadly defined as the modification of seismic waves as they propagate to Earth’s surface (Thompson et al., 2009). There have been many ways proposed to quantify this phenomenon (Boore, 2004). One such measure that has gained in popularity because of its relative ease is the horizontal:vertical spectral ratio (HVSR) of ambient seismic noise (Nogoshi and Igarashi, 1971). Numerous studies have demonstrated that site resonant frequency, a key parameter of site response, can be well defined by HVSR (Bard, 1999). Site amplification as observed in earthquake response spectra tends to be less resolvable through

HVSR relative to methods that compare across multiple stations (see Bard (1999) and references therein).

We use a multimethod surface acquisition approach to characterize V_s versus depth (V_s profiles) at 16 portable seismograph sites deployed as part of aftershock investigations following the August 2011 Mineral earthquake (e.g., McNamara et al., this volume; Chapman, 2013). We acquire horizontal shear (SH) body-wave reflection and refraction data, active-source multichannel analysis of surface-wave data, and passive refraction microtremor (ReMi) data to investigate V_s of the shallow subsurface to bedrock depth and to explore the applicability of several proxy methods for estimating site effects (such as the relationships between V_{s30} , surface geology, HVSR, and site frequency). From the 45 deployed portable seismograph stations, we selected our sites based primarily on: (1) mapped surface geologic units, (2) areal distribution around the main shock epicentral location, and (3) the availability of information from observed HVSR results (see McNamara et al., this volume) for comparison to site effects predicted from the multimethod modeling results.

GENERALIZED SURFACE GEOLOGY

The regional surface geology of the Central Virginia seismic zone and the 2011 M_w 5.8 Mineral earthquake epicentral region consists of Proterozoic–Paleozoic metamorphic rocks that can be broadly categorized into three mapped units for purposes of site characterization. From east to west (Fig. 1), these units include the Goochland terrane, the Chopawamsic Formation, and the Mine Run Complex (e.g., Bailey and Owens, 2012; Hughes et al., 2013). The Goochland terrane consists primarily of Proterozoic–Paleozoic felsic gneiss and associated units, the Chopawamsic Formation consists of Paleozoic metavolcanics and metasediments, and the Mine Run Complex is composed primarily of Paleozoic mélangé. The regional northeast-southwest tectonic fabric is generally evident in the unit contacts.

Although all three units are similar in composition and age, each are likely exposed to locally variable surface weathering that can cause variable soil-site conditions. Five of our V_s sites were acquired on deposits of the Goochland terrane, nine were on deposits of the Chopawamsic Formation, and two were on deposits of the Mine Run Complex (Fig. 1). The geology of the study area is complex in both the overarching lithologic character and in postdepositional alteration through episodic periods of metamorphic and tectonic processes (e.g., Çoruh et al., 1988; Hatcher et al., 1988; Pratt et al., 1988; Lampshire et al., 1994), and weathering processes that likely caused the development of saprolitic deposits (e.g., Odum et al., 2013).

V_s SITE CHARACTERIZATION DATA ACQUISITION AND ANALYSES

Our multimethod V_s characterization approach requires the acquisition of both body-wave and surface-wave data to characterize the subsurface at each site. A key advantage of this

Ground-motion site effects from multimethod shear-wave velocity characterization

approach is that it captures independent wavefield propagation effects that can potentially yield a more robust estimate of the shallow subsurface. We acquired active-source data on 72-sensor linear arrays of both vertical (P-wave reflection and refraction, multichannel analysis of surface waves, or MASW, and ReMi) and SH single-component (SH-wave reflection/refraction) 4.5 Hz resonant-frequency geophones. The vertical and horizontal geophones were collocated at stations spaced at 1.5 m, giving an array aperture of 106.5 m per record. We used a 4.5 kg sledgehammer to impact (1) a steel plate for P-wave energy, and (2) both ends of a horizontal wood timber for SH-wave generation. Data were stacked in the field with generally four impacts recorded at each source location. We also acquired passive linear-array data on the vertical-component sensors, nominally recording 10 30 s records per site. Representative SH-wave field records and frequency-slowness plots of ReMi and MASW records are shown in Figure 2.

Vs from Rayleigh Wave Dispersion Methods

Both MASW and ReMi data were preprocessed with (1) a trace-equalization gain correction to balance trace-to-trace amplitudes, and (2) a centering correction to mitigate high-amplitude noise bursts. The centering function averaged out any deviations or spikes in the data, thus preventing high-amplitude near-offset traces from dominating the spectra. Both the MASW and ReMi techniques as implemented here relied on forward modeling of the dispersion data using proprietary software (SeisOpt-ReMi software by Optim Software, Incorporated) to obtain a best-estimate Vs profile.

ReMi

Louie (2001) introduced the ReMi technique for obtaining Vs from ambient noise surface-wave dispersion obtained on a linear array. The method is popular in site characterization studies because of its simplicity and general effectiveness in comparison to downhole and linear-array active-source methods (Asten and Boore, 2005; Moss, 2008). The analysis of ReMi data relies on the assumption that the propagating surface-wave energy from ambient noise is isotropic and omnidirectional. Louie (2001) and Mulargia and Castellaro (2008) described how these assumptions do not adversely affect results when approximately met. However, at sites where this ambient surface-wave energy does not propagate onto the array omnidirectionally, the result can be an overestimate of the true average site Vs (Zywicki, 2007; Rosenblad and Li, 2009; Strobbia and Cassiani, 2011). For cases where there is a single dominant noise source, the linear sensor array must be in line with and analyzed like an active-source (MASW) data set for the derived apparent velocity to be representative of the true subsurface velocity. In our investigation, sites were selected in part to avoid obvious dominant noise sources, for example, air conditioners and construction sites.

As recommended by Louie (2001), we picked ReMi dispersion data in the slowness-frequency (p - f) domain at the lowest reasonable velocity points, where the p - f spectrum exhibits an observable increase in amplitude out of background noise (Fig. 2A). At each picked frequency we selected three dispersion points to bound an acceptable slowness range to help mitigate picking uncertainty. The picked dispersion data were then forward modeled to obtain one-dimensional (1-D) Vs profiles at each site. The preferred model was obtained through empirical

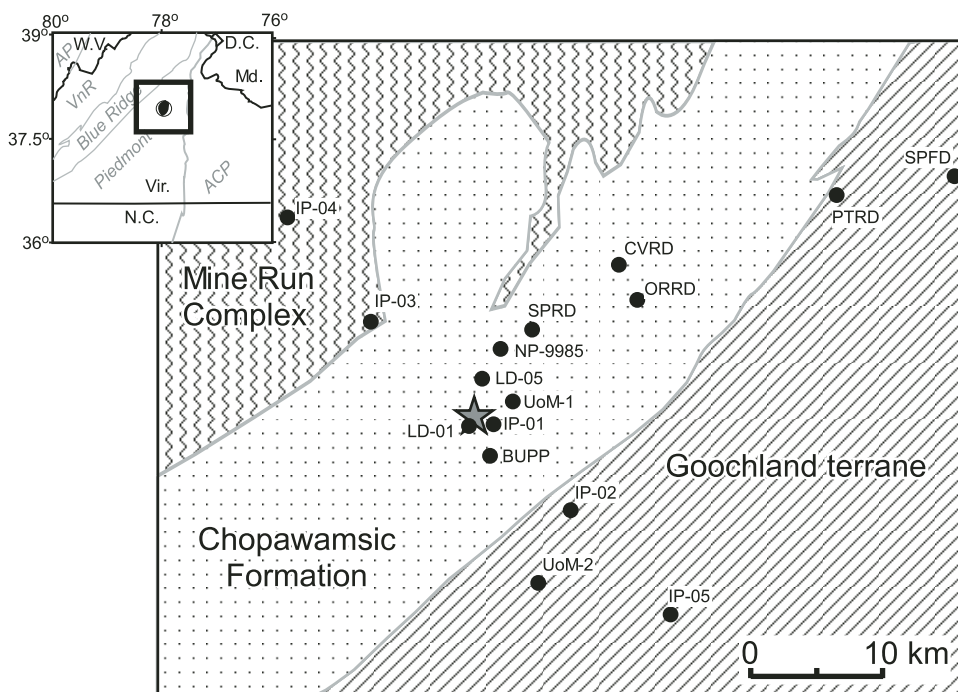


Figure 1. Map of the epicentral region for the 2011 M_w 5.8 Mineral, Virginia, earthquake with locations of 16 portable aftershock stations investigated for site characterization. Contacts between three primary surface geologic units (Mine Run Complex, Chopawamsic Formation, and Goochland terrane) are shown by heavy gray lines (modified from map of R. Harrison, U.S. Geological Survey, 2012, personal commun.). Gray star is epicentral location. Inset: Regional setting for study area. Heavy black rectangle outlines perimeter of investigated region. Generalized physiographic provinces (Bingham, 1991) are shown in gray: ACP—Atlantic coastal plain, AP—Appalachian Plateau, VnR—Valley and Ridge. Focal mechanism for Mineral earthquake is shown. W.V.—West Virginia, D.C.—District of Columbia, N.C.—North Carolina, Vir.—Virginia, Md.—Maryland.

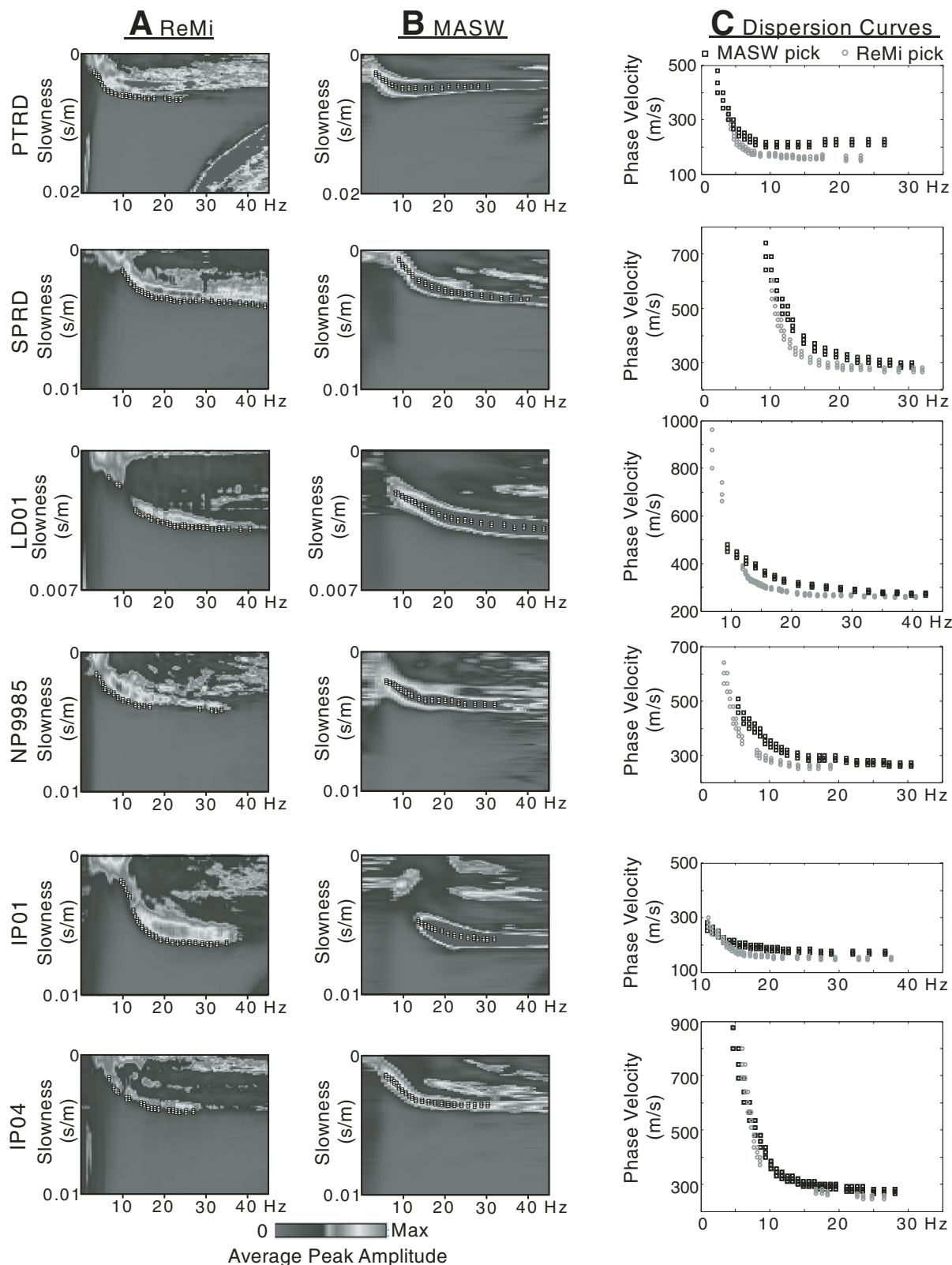


Figure 2 (Continued on facing page). Six representative examples of site characterization data. (A) ReMi (refraction microtremor) frequency-slowness plots analyzed for sites PTRD, SPRD, LD01, NP9985, IP01, and IP04. (B) MASW (multichannel analysis of surface waves) frequency slowness for same sites. Frequency-slowness dispersion picked on A and B are shown by white squares. (C) Comparison of ReMi and MASW picks in frequency-phase velocity domain. MASW picks are black squares and ReMi picks are gray circles. (D) SH (horizontal shear) body-wave field records (traces at common offsets with opposite polarities are overlain for interpretation). Distance from source to end of array in meters is shown on the horizontal axis. Source locations are at 0 m marks on each end of the seismic record display. The first arrival traveltimes are shown along white line tracks.

Ground-motion site effects from multimethod shear-wave velocity characterization

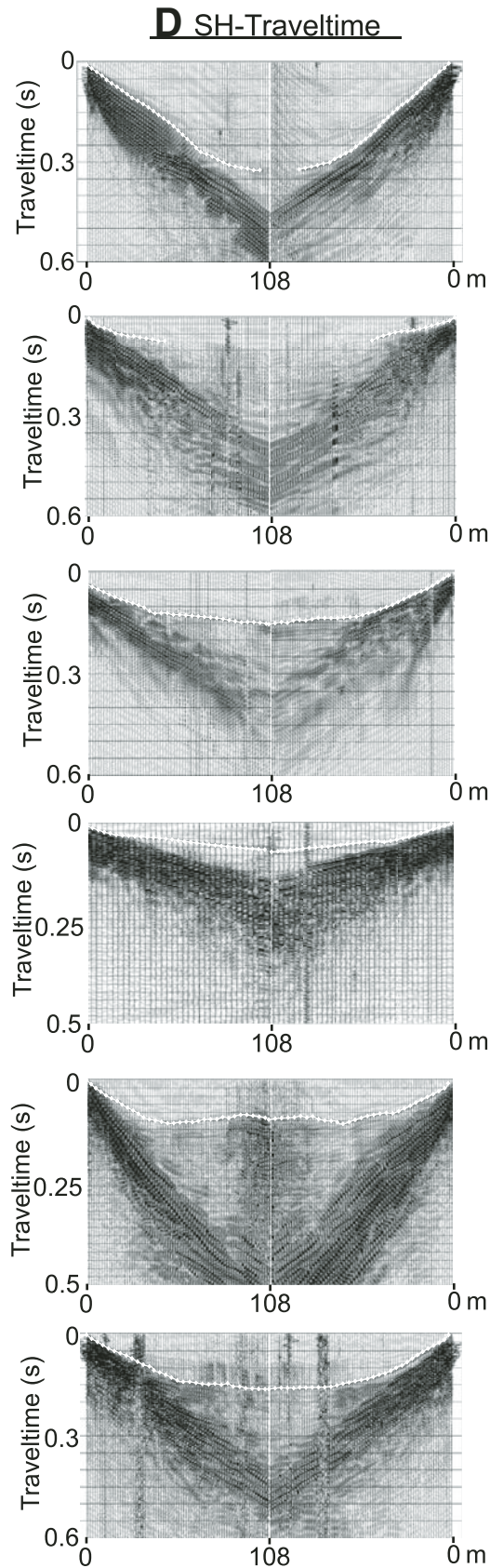


Figure 2 (Continued).

sensitivity testing of the model parameters. Model uncertainties were commonly $\pm 10\%$ at the surface increasing to generally $\pm 20\%$ at the maximum depth of investigation (commonly the bedrock surface).

MASW

The MASW surface acquisition technique was introduced by Park et al. (1999) for obtaining V_s from surface-wave dispersion analysis. The method has been proven to be effective for V_s site characterization when compared against downhole V_s logging (Xia et al., 2002; Stephenson et al., 2005; Foti et al., 2011). MASW is an active source technique, which by definition relies on an external source, in our case a sledgehammer, to generate the surface waves (most commonly Rayleigh waves) for analysis. Passive-source MASW (e.g., Park and Miller, 2008), and interferometric MASW (O'Connell and Turner, 2011) are more recent extensions of the traditional MASW technique.

We acquired MASW data with the identical receiver array used to obtain data for ReMi analysis. We acquired data with source impacts at every third station, nominally, for detailed Rayleigh-wave analysis. It is interesting that the optimal field records selected for MASW analysis were consistently from mid-array source locations. These yielded the best-quality p-f domain records for analysis (Fig. 2B). This may indicate a lack of source power from the sledgehammer and/or a high degree of multidimensional variability of the subsurface. In addition, we analyzed all offsets from maximum aperture (to 54 m) to as small as 1.5 m; this is not standard practice because of the likely presence of surface-wave near-source propagation effects (e.g., Park et al., 1999). However, we ensured minimal impact from these near-source effects by limiting the frequency band used in the analysis (e.g., Foti et al., 2011).

The p-f domain analysis conducted on the MASW data was similar to that of ReMi, except that the dispersion picks followed the peaks of the p-f spectral image (Figs. 2A, 2B). Because the source of the surface-wave energy was known, the fundamental-mode amplitude peak was assumed to be the correct dispersion curve location. The sledgehammer source generated higher frequency surface-wave energy than was generally observed in the ambient noise data; this is evident from comparison of the phase velocity plots in Figure 2C above ~ 20 Hz. Both the ReMi and MASW data lacked low-frequency signal below ~ 4 Hz, although this did not adversely affect the depth of investigation for this study because bedrock was typically shallow.

V_s from SH Body-Wave Traveltimes

We manually picked first arrival traveltimes from the SH body-wave data for each of the 16 sites after applying a trace amplitude correction; no additional preprocessing such as band-pass filtering was necessary (see representative records in Fig. 2D). No distinct SH-wave reflections were identified in these data except at site UoM2, where the reflector was used to constrain bedrock depth at 55 m. No velocity inversions were evident

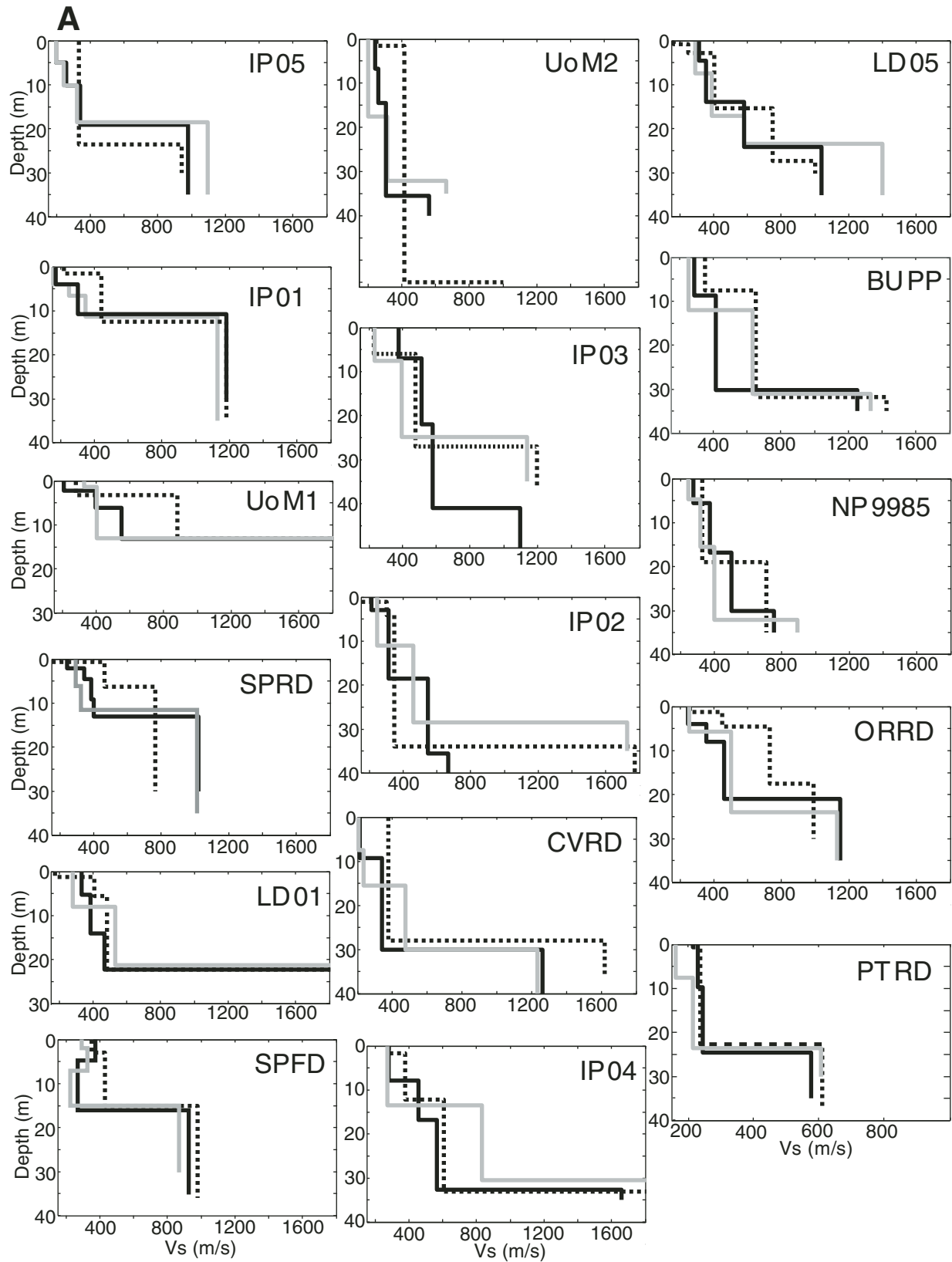


Figure 3. (A) Shear-wave velocity versus depth (V_s) profiles for the three surface acquisition methods interpreted at each of the 16 investigated sites. Profiles represent best-fit parsimonious solutions, with the minimum number of V_s layers needed to fit the respective data set. Uncertainties are typically $\pm 10\%$ for the upper 10 m and $\pm 20\%$ at maximum depth of investigation. The gray line is the ReMi (refraction microtremor) model, the solid black line is the MASW (multichannel analysis of surface waves) model, and the dashed black line is the SH (horizontal shear) body-wave model. All plots have common V_s scales except for site PTRD. (Continued on facing page).

Ground-motion site effects from multimethod shear-wave velocity characterization

(e.g., Williams et al., 2003), and thus the picked traveltimes were interpreted as direct arrival and refraction phases. We developed models with the fewest layers that give an optimal fit to the observed data (parsimonious solution). We first developed an initial 1-D Vs model using a conventional slope-intercept analysis (e.g., Mooney, 1984) incorporating a robust linear regression for estimating layer velocities and intercept times (robust regression analysis was performed using the MATLAB function `robustfit`; www.mathworks.com/). This initial model was next refined through the RAYINV2 two-dimensional ray tracing and damped least-squares inversion process of Zelt and Smith (1992). Although this second-stage modeling was 2-D, we constrain the model to be a best-fit 1-D approximation from the SH body-wave data. With the exception of site UoM2 these data suggest shallow (<40 m) bedrock sites with increasing Vs with depth (Fig. 3).

Modeling Procedures

While published studies have demonstrated varying degrees of success on the joint modeling of multimethod data sets for site characterization (Ivanov et al., 2006; Dal Moro and Pipan,

2007; Chang et al., 2011; Odum et al., 2013), there are significant impediments to obtaining such a solution. In recent years Bayesian and Monte-Carlo inverse modeling approaches for obtaining Vs have gained popularity (e.g., Dal Moro and Pipan, 2007; Molnar et al., 2010; Socco et al., 2010), but a standardized modeling approach for multimethod data sets with multiple wavefield components is currently lacking. In addition to methodological uncertainties in imaging the subsurface, as discussed previously, propagation effects such as seismic anisotropy, where wave speed differs by propagation direction (e.g., propagating seismic energy may experience anisotropic effects in two horizontal as well as vertical directions) can play a role in estimating Vs and therefore in jointly modeling horizontally propagating (SH body wave, Love wave) and Rayleigh wave (ReMi, MASW) data sets. Measured variation in shear-wave anisotropy is commonly as high as 5% between fast and slow directions (e.g., Crampin and Lovell, 1991), with values as high as 12% reported in the upper 30 m (Harris, 2005). Clearly, wavespeed variations in this range can adversely affect modeling results with multimethod data sets.

For this investigation we interpreted and modeled data sets from each of the three methods independently, then we compared

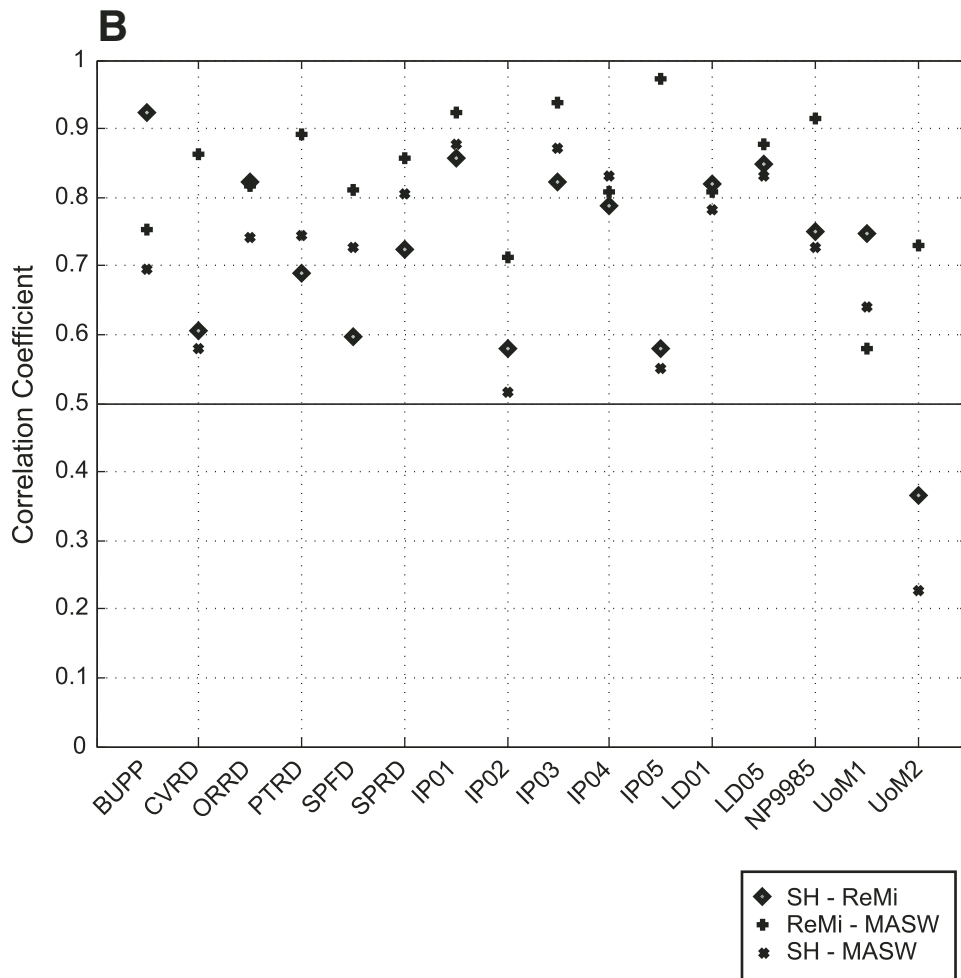


Figure 3 (Continued). (B) Kendall tau correlation coefficients between SH body-wave and ReMi models, SH body-wave and MASW models, and ReMi and MASW models.

the best-fit Vs models, Vs30, interpreted bedrock depth, and estimated site frequency for each site. As described herein, the surface-wave dispersion data were modeled using proprietary forward-modeling software, while SH body-wave data were both forward and inverse-modeled with open-source codes. During forward modeling, both layer depth and layer Vs were varied to optimize the best-fit solution. We emphasize that we did not interpret these data blind relative to each other; however, we objectively assessed goodness of model fits for each data set independent of model parameters from other data sets. The best-fit model for each method at each site is listed in the Appendix.

COMPARISON OF Vs PROFILES

Defining seismic bedrock (henceforth bedrock) as the first model layer with Vs > 760 m/s (e.g., Building Seismic Safety Council, 2000), bedrock depths qualitatively have good agreement at seven sites (BUPP, CVRD, SPFD, IP01, IP04, IP05, and LD01), as shown in Figure 3A. At the remaining sites either the interpreted bedrock depths differ by as much as 60% from the median value or seismic bedrock depth was not reached. Bedrock Vs is consistently interpreted between 1000 m/s and 1800 m/s, which is a reasonable range for the igneous intrusive, metasedimentary, and metavolcanic rocks underlying the region at shallow depth (<100 m). At some sites poor constraint on bedrock Vs is primarily caused by lack of sufficiently far-offset traveltimes in the SH body-wave data and by a lack of sufficiently long wavelengths in the surface-wave data sets.

Overall, based on visual inspection the three Vs profiles generally agree at eight of the sites (IP01, IP03, IP04, IP05, LD01, LD05, NP9985, PTRD). At the remaining sites at least one of the profiles diverges from the general trend of Vs versus depth to the interpreted bedrock interface. Vs of the overburden varies from ~200 m/s at the ground surface to ~600 m/s at the depth of the bedrock surface. At site SPFD surface-wave methods suggest a velocity inversion between ~5 and 15 m depth that is not resolved in the body-wave model; however, bedrock depth is common among all three methods. This site is notable because it was the most urbanized of our sites and was affected by significant traffic and cultural noise, which affected signal quality on all data sets and made interpretation of the active-source methods the most difficult of any sites presented here.

To obtain a more quantitative assessment of the similarity between the preferred models at each site we conducted a Kendall tau rank correlation test (e.g., Kendall, 1970), which is a non-parametric measure that gives an estimate of statistical dependence between two variables. Values of this parameter range between -1 (perfect inverse correlation) to 0 (no correlation) to 1 (perfect correlation). To conduct this coefficient estimation each Vs profile was discretized at 1 m intervals to the maximum depth of interpretation for the shallowest profile at a given site. The correlation values (Fig. 3B) suggest that profiles at only five sites have interprofile pairs below 0.6, which suggests good correlation, or similarity, between the derived model results. The site

with the lowest overall similarity is site UoM2, while the highest correlation coefficient (most similar) was between the ReMi and MASW models at site IP05.

Vs30, BEDROCK DEPTH, SITE FREQUENCY, AND OBSERVED HVSR

In addition to the interpreted bedrock depth, we estimated Vs30 and site frequency for each of the preferred Vs profiles, to be used as measures for comparison to observed HVSR and surface geology. We calculated Vs30 using the equation:

$$V_{sz} = \frac{\sum_{i=1}^n d_i}{\sum_{i=1}^n (d_i / V_{s_i})}, \quad (1)$$

where d_i and V_{s_i} are the layer thickness (in meters) and shear-wave velocity of the i^{th} layer, respectively, and z is the depth of averaging (Building Seismic Safety Council, 2000). Although site-specific seismic amplification is often too complex to be solely predicted from Vs30 (Harmsen, 1997; Wald and Mori, 2000; Frankel et al., 2002; Castellaro et al., 2008), this parameter is widely used to account for site conditions by the earthquake engineering community and to estimate potential earthquake ground motions at building sites (International Code Council, 2006). Because Vs30 is a ubiquitous parameter used for site characterization, we used it for comparative purposes even in cases where bedrock depth was shallower than 30 m.

Using our definition of bedrock depth as the layer boundary below which Vs is 760 m/s or greater, we interpreted the bedrock contact at all sites but PTRD. Bedrock depth at site UoM2 is estimated from only the SH body-wave interpretation. Site period has been discussed as a better proxy for site effects than Vs30 (e.g., Zhao and Xu, 2013). Thus, in addition to calculating Vs30, we calculated site frequency (inverse of site period) by: (1) setting z in Equation 1 to interpreted bedrock depth, (2) calculating the average velocity to depth z , and (3) dividing the resultant V_{sz} by four (i.e., one-quarter wavelength; see Joyner et al., 1981) to obtain the estimate. Site frequency is the effective spectral value at which site resonance should occur based on the interpreted bedrock depth and time-averaged Vs of the overlying soil column. An alternative site response modeling approach to this one-quarter wavelength approximation would be calculation of the SH transfer function through the Vs profile (e.g., Odum et al., 2013). The fundamental resonance frequency obtained through transfer-function modeling is generally equivalent to the frequency obtained through site frequency calculation (for an overview and comparison of the one-quarter wavelength and SH transfer-function modeling approaches, see Boore and Brown, 1998).

Vs30 Compared to Surface Geology

The Vs30 values from each of the three surface-seismic methods are calculated for each site and categorized by the

Ground-motion site effects from multimethod shear-wave velocity characterization

three principle surface-geologic units (Fig. 4; Table 1). With the exception of one measurement, at site UoM1, all Vs30 values are within the NEHRP site classes C and D; median values tend to be site class C. Vs30 of the SH body-wave and ReMi data were highest and lowest, respectively, at 10 of the sites. Among the surface geologic units the three methods matched most closely on the Mine Run Complex, although we acquired data at only two sites for this unit.

Based on visual inspection, Vs30 measurements on the Chopawamsic Formation are somewhat higher across the epicentral region; however, the limited number of sites does not allow for a definitive correlation. The greatest overall variation between Vs30 values was for sites on the Chopawamsic Formation, where Vs30 derived from SH body-wave analysis was highest on six of the nine sites and was the median value at the remaining three. Vs30 acquired on the Goochland terrane sites tended to be lower, with three of the five sites being site class D. Overall, no clear correlation between Vs30 and geology can be discerned from these data; this is consistent with the common age and composition of the surface geologic units and with exposure to similar weathering effects. Thus, given how the surface geologic units

are defined herein, these data suggest that using surface geology as a proxy for Vs30 or for site effects would not be a reliable approach across the Mineral earthquake epicentral region.

Bedrock Depth and Site Frequency Compared to Surface Geology

Similar to variations observed in Vs30 across the region, the interpreted depth to bedrock does not vary substantially across the epicentral region, based on mapped surface geology (Fig. 5). Interpreted bedrock depth varied from 3 m to 55 m; median values ranged from 11 m to 34 m. With the exception of site UoM2, where only a single method was interpreted as reaching bedrock (although both surface-wave methods also suggest that bedrock is 35 m or deeper), the majority of the interpreted bedrock depths are between 10 m and 40 m. The lack of variability in the interpreted bedrock depth might be related to the common Paleozoic age of all surface units and a probably similar weathering history.

In Figure 6, we plot observed HVSr calculated from ambient noise at nearby portable seismograph sites versus median

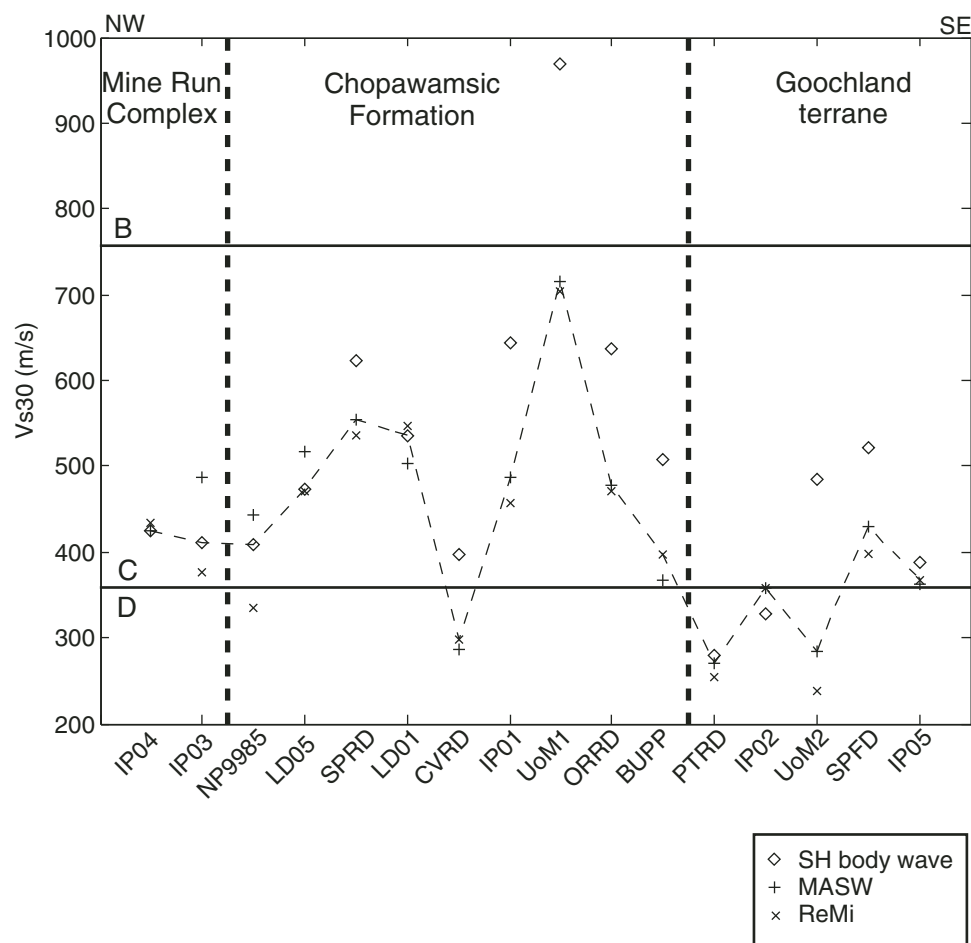


Figure 4. Vs30 (time-averaged shear-wave velocity to depth of 30 m) values from the three methods calculated for each site. Sites are grouped by generalized surface geologic units and are presented, from left to right, by approximate projection onto a northwest-southeast transect through epicenter. Heavy black dashed vertical lines are boundaries of the surface geologic units. Vs30 from SH (horizontal shear) body wave, ReMi (refraction microtremor), and MASW (multichannel analysis of surface waves) are shown; median values at each site are connected by the thin dashed line. Boundaries between National Earthquake Hazards Reduction Program site classes B-C and C-D (Building Seismic Safety Council, 2000) are shown by horizontal black lines; all sites investigated here are either median class C or D (Table 1).

TABLE 1. Vs30 CALCULATED FOR THREE METHOD INTERPRETATIONS AT 16 SITES IN VIRGINIA

Site	Latitude (°N)	Longitude (°W)	SH body (m/s)	ReMi (m/s)	MASW (m/s)	Median site class	Distance to station (m)
BUPP	37.935001	77.914545	508	397	368	C	35
CVRD	38.067870	77.807805	396	297	287	D	83
ORRD	38.043912	77.790218	637	472	478	C	56
PTRD	38.119908	77.622937	280	254	271	D	41
SPFD	38.135464	77.521247	522	397	430	C	8
SPRD	38.022860	77.879688	624	536	554	C	71
IP01	37.956321	77.911358	643	457	488	C	25
IP02	37.899217	77.840705	327	357	357	D	55
IP03	38.020878	78.014543	411	376	488	C	35
IP04	38.091381	78.093652	425	435	424	C	102
IP05	37.830480	77.756429	387	366	362	C	70
LD01	37.954878	77.933288	536	547	504	C	40
LD05	37.986336	77.921549	474	471	518	C	23
NP9985	38.010084	77.908152	409	336	444	C	63
UoM1	37.971620	77.895993	968	703	715	C	85
UoM2	37.846773	77.871070	484	238	283	D	240

Note: Median Vs30 (shear-wave velocity to a depth of 30 m) in bold. Site class based on median Vs30. Distance to station is approximate distance from surface array midpoint to portable seismograph station. SH—horizontal shear wave; ReMi—refraction microtremor; MASW—multichannel analysis of surface waves.

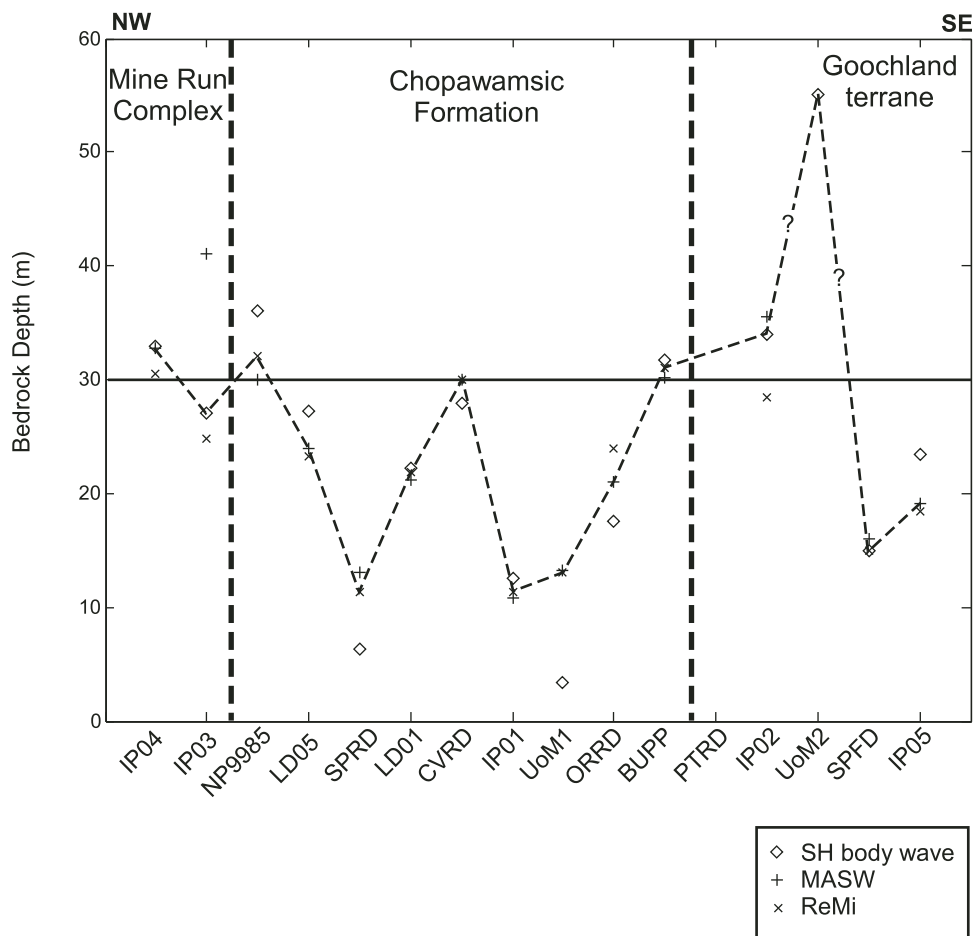


Figure 5. Interpreted bedrock depth grouped by generalized surface geologic units. Sites are shown by approximate projection onto northwest-southeast transect through epicenter (from left to right). Heavy black dashed vertical lines are boundaries of the surface geologic units. Interpreted bedrock depth from SH (horizontal shear) body wave, ReMi (refraction microtremor), and MASW (multichannel analysis of surface waves) are shown; median values at each site are connected by the thin dashed line (queried to site UoM2 because only one bedrock depth interpreted at this site).

Ground-motion site effects from multimethod shear-wave velocity characterization

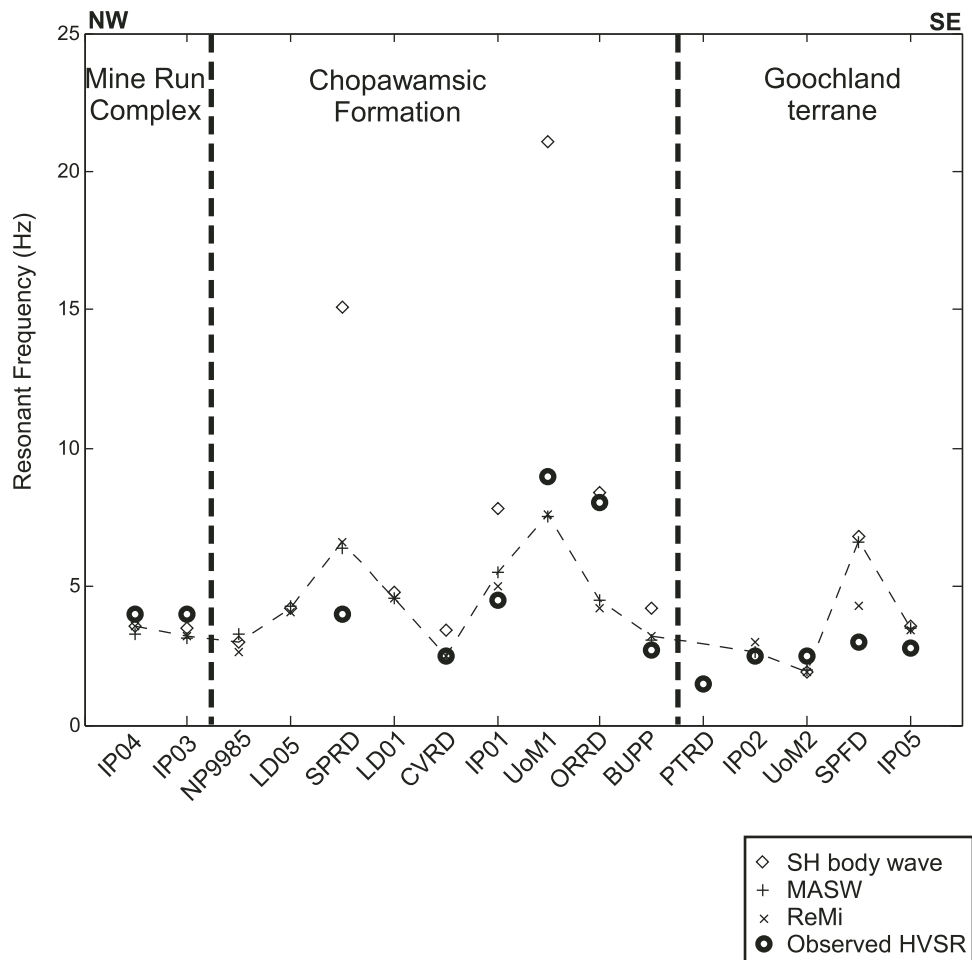


Figure 6. Site frequencies calculated for each site grouped by generalized surface geologic units. Sites are shown by approximate projection onto northwest-southeast transect through epicenter (from left to right). Site frequency calculated from SH (horizontal shear) body wave, ReMi (refraction microtremor), and MASW (multichannel analysis of surface waves) are shown; median values at each site are connected by the thin dashed line. HVSr (horizontal:vertical spectral ratios) resonant frequencies observed at 13 of the portable seismograph sites are shown.

site frequency calculated from average V_s for the interpreted bedrock depth at the 15 sites where we interpret bedrock based on $V_s > 760$ m/s (Table 2). HVSr peak resonant frequencies at 13 of these 15 sites have been calculated (McNamara et al., this volume). The observed frequencies tend to be between 4 and 5 Hz over the northwesternmost four sites, showing minimal correlation with the surface geologic unit. Observed HVSr resonant frequencies over the southeasternmost six sites were between 2 and 4 Hz. Median site frequencies generally were between 3 and 7 Hz. While ideally we want HVSr and site frequency to match, many features between these data match qualitatively, including the rise in frequency between sites CVRD and BUPP, and nominal range and flatness in resonance to the northwest (sites IP03 and IP04).

V_{s30} Compared to HVSr

We next compare V_{s30} to observed HVSr at the 13 sites where there are reliable HVSr calculations from ambient noise recorded at nearby portable seismographs. We can make only limited determinations about correlation between V_{s30} and HVSr because this is a data set with limited number of observa-

tions; however, inspection reveals a general linear relationship, as shown in Figure 7. This linear relationship, as determined through a robust linear regression, suggests a standard error of ~ 58 m/s, which in practice could mean a large uncertainty in assigning site classification based on observed HVSr resonant frequencies; however, the calculated V_{s30} is within 5% of the predicted value at seven of the sites.

Bedrock Depth and Site Frequency Compared to HVSr

As shown in Figure 8, a distinct negative slope to the regression of the median bedrock depths and HVSr values was observed at the 12 usable sites for this analysis. Such a negative correlation is consistent with higher HVSr frequencies correlating with shallower bedrock. However, three sites with interpreted median bedrock depths between 10 and 13 m and HVSr resonant frequencies between 3 and 5 Hz are at depths more than 50% shallower than the regression line through this frequency range. Thus, using our site characterization regression model, bedrock depth would be overpredicted and V_{sz} underpredicted, possibly causing bias in site class estimation.

TABLE 2. INTERPRETED BEDROCK DEPTH AND SITE FREQUENCY CALCULATED FOR THREE METHOD INTERPRETATIONS AT 15 SITES IN VIRGINIA

Site	Bedrock Z SH body (m)	Bedrock Z ReMi (m)	Bedrock Z MASW (m)	Fs SH body (Hz)	Fs ReMi (Hz)	Fs MASW (Hz)	Observed HVSR (Hz)
BUPP	31.8	31	30.3	4.24	3.24	3.05	2.7
CVRD	28	30	30	3.4	2.5	2.4	2.5
ORRD	17.5	24	21	8.4	4.2	4.5	8
PTRD	---	---	---	---	---	---	1.5
SPFD	15	15	16	6.8	4.3	6.6	3
SPRD	6.3	11.5	13	15.1	6.6	6.4	4
IP01	12.5	11.3	10.8	7.8	5	5.5	4.5
IP02	34	28.5	35.5	2.5	3	2.6	2.5
IP03	27	24.8	41	3.5	3.2	3.1	4
IP04	33	30.5	32.7	3.6	3.6	3.3	4
IP05	23.5	18.5	19.1	3.6	3.4	3.5	2.8
LD01	22.2	21.9	21.3	4.8	4.6	4.6	---
LD05	27.2	23.3	24	4.2	4.1	4.3	---
NP9985	36	32	30	3	2.6	3.3	---
UoM1	3.3	13	13.3	21.1	7.6	7.5	9
UoM2	55	---	---	1.9	---	---	2.5

Note: Median bedrock depth (Z) and site frequency (Fs) in bold. Observed HVSR (horizontal:vertical spectral ratios) at 13 sites where ambient noise analysis available. SH—horizontal shear wave; ReMi—refraction microtremor; MASW—multichannel analysis of surface waves. Dashes indicate no value is interpreted (or calculated) for a given site-method pair.

Ideally there should be a strong correlation between calculated site frequency and observed HVSR. We use the Vs profile with the median interpreted bedrock depth at each site for calculation of the preferred site frequency. At seven of 12 sites the method with median bedrock depth also gives the median site frequency, but at five sites the median site frequency differs from the value used in this analysis (Table 2). Although our analysis is limited to

12 data points, we observe a moderate correlation between these parameters (Fig. 9). The best-fit robust linear regression trends through these data with a slope that is gentler than unity. This regression line has a zero intercept of 1.5 Hz and a sigma error of 1.26. While the regression spans the frequency band of interest in most site response analyses (between 0 and 10 Hz), we lack information between 0 and 2 Hz as well as between 5 and 8 Hz

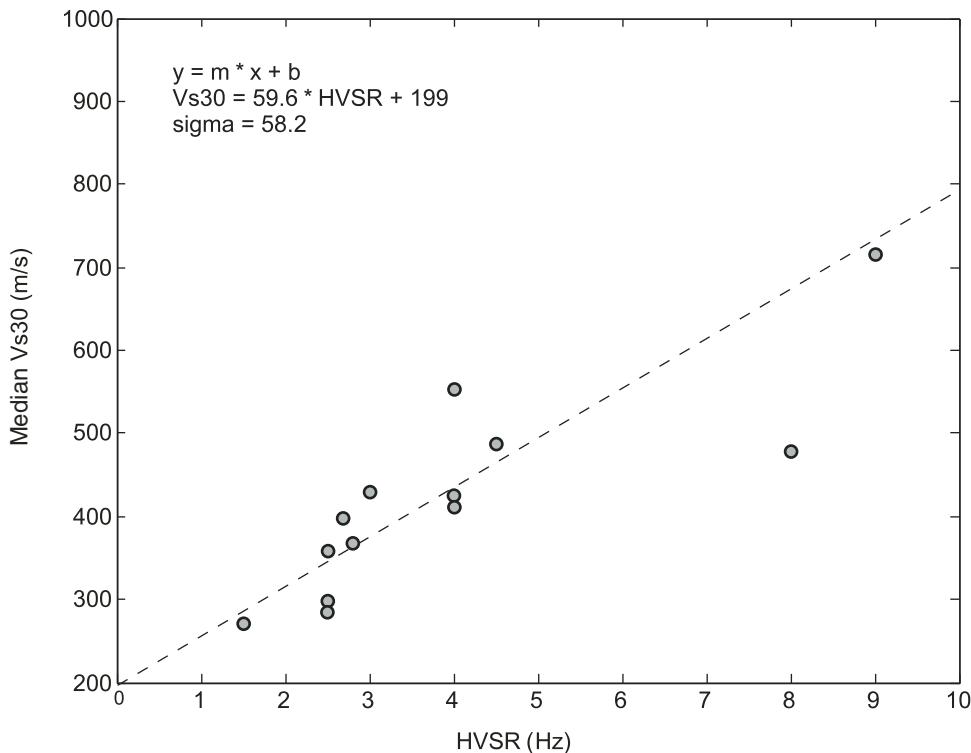


Figure 7. Vs30 (time-averaged shear-wave velocity to depth of 30 m) versus interpreted versus observed HVSR (horizontal:vertical spectral ratios) peak frequencies at 13 sites. Linear regression, black dashed line, has a standard error of ~58 m/s and is most valid in the range 1.5–9 Hz.

Ground-motion site effects from multimethod shear-wave velocity characterization

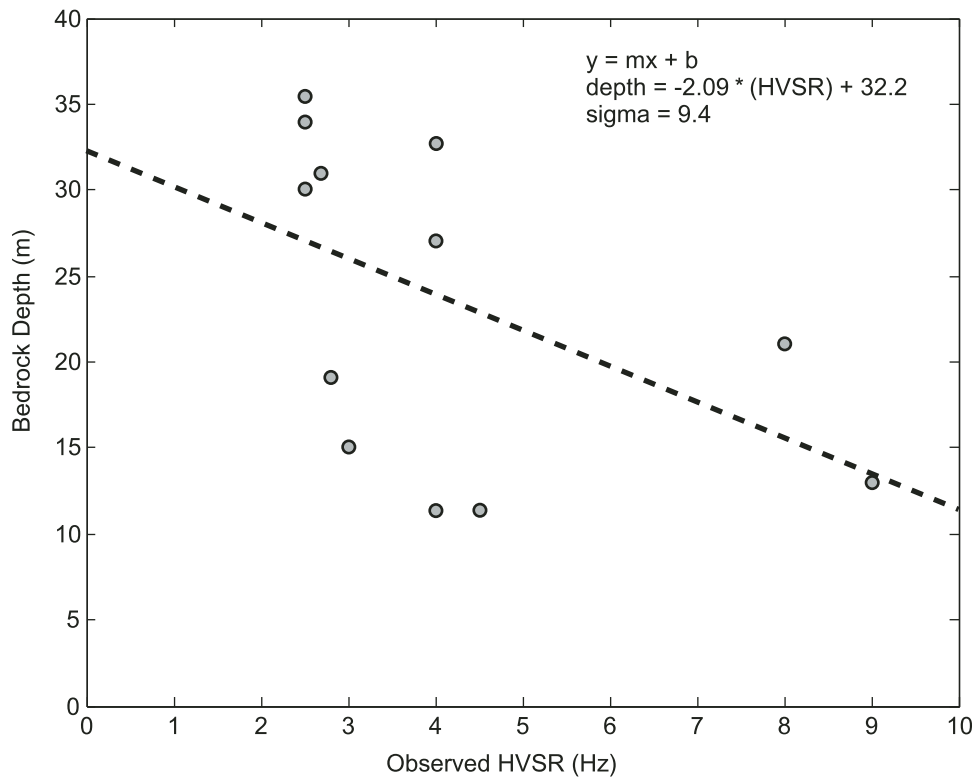


Figure 8. Bedrock depth versus observed HVSR (horizontal:vertical spectral ratios) peak frequencies at 12 sites. A distinct negative slope to regression is consistent with higher HVSR frequencies correlating with shallower bedrock.

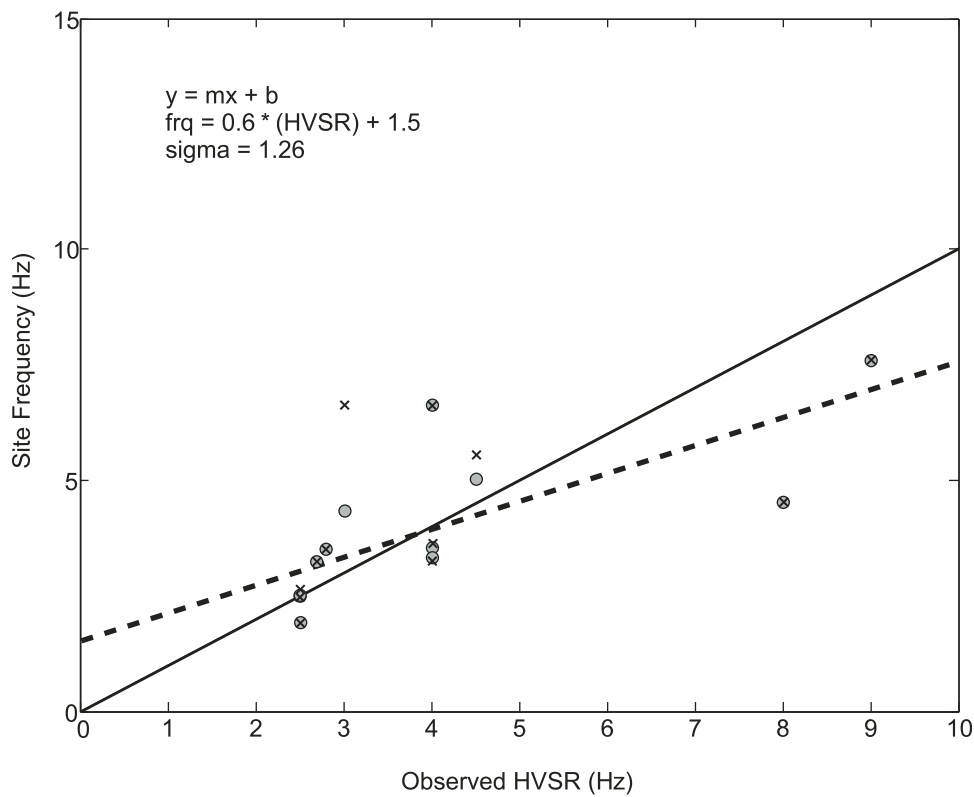


Figure 9. Site frequency (frq) versus observed HVSR (horizontal:vertical spectral ratios) at 12 sites where both interpreted bedrock depth and HVSR resonant frequencies are available. Solid black line is unity (perfect match between site frequency and observed HVSR). Gray circles are the preferred site frequencies calculated from V_s (shear-wave velocity versus depth) profiles with median bedrock depth; x values are median site frequencies, which differ from preferred values at five sites. Robust linear regression shown by dashed line and is best fit with standard error of 1.26 Hz.

that could critically constrain the dependence between observed HVSR and calculated site frequency across the epicentral region.

As a further test of the regional correlation between site frequency and V_{s30} versus observed HVSR, we calculate Kendall tau coefficients for site frequency and V_{s30} of 0.76 and 0.80, respectively; this suggests that both parameters are moderately correlated to HVSR and that V_{s30} is marginally more correlated than site frequency for these data. When tested against a null hypothesis (no correlation with HVSR, or $\tau = 0$) through permutation testing, both site frequency and V_{s30} showed statistically significant correlation to observed HVSR over the null hypothesis (0.0013 and 0.0003, respectively).

DISCUSSION

We believe that results from this study have implications for Central Virginia seismic zone and eastern U.S. ground motions. Analysis of our Vs profiles including regressions with observed HVSR gives us some confidence to their application as site effect predictors in the central Virginia epicentral region; however, our regression analysis may not yield reliable site effects estimates outside the Central Virginia seismic zone or when extrapolating site classification onto surface geologic lithologies dissimilar to those encountered across the epicentral area. NEHRP site classes C and D may be prevalent throughout central Virginia external to the Atlantic coastal plain (Fig. 1).

Uncertainties in Vs for Surface Acquisition Methods

Site location can introduce inherent uncertainties in developing 1-D Vs profiles. The active- and passive-source acquisition methods used here required 106.5 m of linear distance for the sensor arrays and at least 1.5 m off each end for the active-source locations. Although the seismic data propagate through and are affected by a large volume of subsurface material, we approximate a 1-D velocity structure during modeling. This assumption becomes less valid with both lateral subsurface geologic and geophysical heterogeneity and with topographic variations (e.g., Socco et al., 2010). Finding an ~130-m-long acquisition site (sufficient space for the array and source equipment operation) at each portable seismograph site was often difficult because of logistical constraints caused by topography and site accessibility. At times, we were required to utilize hummocky pastureland or to acquire our surface data at distances >100 m from the seismograph station (see Table 1; note that these distances are to the array midpoint and that some sensors were commonly closer to the seismograph). Given a choice between acquisition sites, we gave highest priority to those closest to the seismograph stations. At four of the 16 sites, station elevations differed by at least 4 m along the profile. Given a depth of investigation of typically <40 m, this topographic variation can introduce additional uncertainty in developing an average 1-D Vs versus depth model.

Each surface method also has inherent uncertainties, including those caused by (1) limitations in spectral bandwidth of the source,

a problem for both active and passive methods, (2) limitations in resolution, (3) errors introduced in data analysis due to signal quality and interpretation inaccuracy, and (4) the nonuniqueness of the model solution. Although assessing model uncertainty is often site specific and difficult to accomplish, surface methods typically have empirically estimated uncertainty of ~10% at shallow depth, with uncertainty increasing with depth (e.g., Stephenson et al., 2005; Odum et al., 2013). Blind comparisons of downhole Vs logs to both active- and passive-source site characterization methods commonly demonstrate that the average V_{s30} values for all methodologies are consistently within 15% of the logged Vs (Xia et al., 2002; Asten and Boore, 2005).

Despite the range of uncertainties encountered in site characterization studies with noninvasive surface acquisition methods, we believe a multimethod approach such as the three-method analysis we conduct provides an important opportunity to further mitigate possible error. Using a multimethod approach, estimates of site response can be obtained through straightforward calculations, such as the use of median V_{s30} and resonant frequency in our comparisons, which can potentially reveal bias and/or systematic errors of a single method. Furthermore, as shown in Figure 6 predicted site frequencies for an individual method, although rare, differed from the observed HVSR by as much as a factor of 3.8, whereas the multimethod median site frequency was commonly within 25% of the observed; this result is a compelling reason to use a multimethod approach as advocated here.

Predicting Site Response from Vs

Boore (2004) presented arguments for the difficulty in predicting site response given the current state of practice in estimating site effects through Vs studies; he noted that site response is difficult to predict because of the inherently large variability in ground motions from earthquake to earthquake, and thus suggested that site response may not be predictable because of large uncertainties in earthquake source effects, path effects, and the indistinct line often encountered in defining a path versus a site effect. However, Boore (2004) also concluded that site classification generally can be useful in distinguishing between site amplifications of different deposits and that using a mean site response for a class of sites, given enough sites and earthquakes, is likely a tractable approach. In our investigation, given the limited number of sites, the median V_{s30} value at each site suggests that NEHRP site classifications are consistently C or D across the three tested geologic units (Fig. 4). The ages of units suggest that variations across the Central Virginia seismic zone region are likely due to differential weathering of the soil and shallow bedrock at the investigated sites, rather than unique properties of the mapped geologic units.

Site Response and Proxy Methods

Defining uncertainties in the relationship between site response and near-surface geology continues to be difficult (e.g., Wald and Mori, 2000; Wills et al., 2000; Tinsley et al.,

Ground-motion site effects from multimethod shear-wave velocity characterization

2004). Similar studies exploring uncertainties in the application of proxy methods for site characterization have shown large variability (Wills et al., 2000; Allen and Wald, 2009; Yong et al., 2012). As noted by Hough (2012), many studies to date suggest significant systematics (in essence, how we go about classifying a given site) in obtaining empirical estimates of site response. While our error analysis was nonexhaustive, we estimate error in the 10%–20% range of average V_s in our site characterization modeling.

Debate over the utility of V_s30 in predicting site response is ongoing (e.g., Castellaro et al., 2008; Yong et al., 2012; Zhao and Xu, 2013). Based on reanalysis of the Borchardt (1994) horizontal amplification data set from the 1989 Loma Prieta earthquake, which helped establish V_s30 as a predictor of site response, Castellaro et al. (2008) concluded that V_s30 appears to be, in fact, a weak proxy for site amplification. Comparison of V_s30 to HVSR from our data suggests a moderate correlation between the observed site effect and the V_s30 parameter.

CONCLUSIONS

We characterize the median V_s30 values between 270 m/s and 715 m/s at 16 sites through the epicentral region of the 2011 M_w 5.8 Mineral earthquake. All of these sites would thus be categorized as NEHRP site class C or D. While we cannot preclude using mapped surface geology as a proxy for site response, we see no compelling evidence for associating different site effect levels with the geologic units as differentiated in this study across the epicentral region: because the units are all Paleozoic in age and have likely had similar weathering histories, their seismic propagation parameters might be expected to be similar. Using

resonant frequencies calculated from ambient noise HVSR as representing an observed fundamental site response parameter, we compare against calculated site frequencies derived from seismic bedrock depth and overlying average versus robust linear regression of HVSR with both site frequency and V_s30 demonstrate moderate correlation to each, and thus both appear to be somewhat representative of site response in this region. Kendall tau non-parametric statistical testing suggests that the site frequency calculated from average V_s to interpreted bedrock depth is a moderately good predictor of site response in this region, as is V_s30 , which is consistent with a significant number of sites having bedrock depth in the 30 m range.

ACKNOWLEDGMENTS

We thank David Worley and Jim Allen for their assistance during field data acquisition. Processing and forward modeling of the ReMi data were performed using SeisOpt-ReMi software by Optim Software, Incorporated. The refraction data traveltimes were interpreted using ProMAX and the slope-intercept method described by Mooney (1984). Seismic reflections were interpreted interactively where possible using ProMAX by Landmark Graphics Corporation. MATLAB is a registered trademark of The MathWorks, Incorporated. (See www.mathworks.com/trademarks for a list of additional trademarks. Other product or brand names may be trademarks or registered trademarks of their respective holders.) Ray tracing and modeling of SH body-wave traveltimes were also conducted with RAYINVR by Zelt and Smith (1992). Any use of trade, product, or firm names is for descriptive purposes only and does not imply endorsement by the U.S. Government.

APPENDIX. V_s VERSUS DEPTH PROFILES FOR THREE METHODS EMPLOYED AT EACH OF 16 PORTABLE SEISMOGRAPH STATIONS

Site	SH body wave		ReMi		MASW	
	V_s (m/s)	Depth (m)	V_s (m/s)	Depth (m)	V_s (m/s)	Depth (m)
BUPP	350	0	255	0	289	0
	350	7.6	255	12	289	8.75
	650	7.6	633	12	415	8.75
	650	31.8	633	31	415	30.25
	1425	31.8	1333	31	1252	30.25
	1425	35	1333	35	1252	35
CVRD	376	0	207	0	214	0
	376	28	207	7.5	214	9.25
	1620	28	233	7.5	339	9.25
	1620	36	233	15.5	339	30
			476	15.5	1263	30
			476	30	1263	45
			1235	30		
			1235	45		
ORRD	256	0	255	0	245	0
	256	1.2	255	5.75	245	4
	448	1.2	503	5.75	356	4
	448	4.5	503	24	356	8
	730	4.5	1129	24	461	8
	730	17.5	1129	35	461	21
	990	17.5			1148	21
	990	30			1148	35

(Continued)

*Stephenson et al.*APPENDIX.Vs VERSUS DEPTH PROFILES FOR THREE METHODS EMPLOYED
AT EACH OF 16 PORTABLE SEISMOGRAPH STATIONS (*Continued*)

Site	SH body wave		ReMi		MASW	
	Vs (m/s)	Depth (m)	Vs (m/s)	Depth (m)	Vs (m/s)	Depth (m)
PTRD	217	0	164	0	232	0
	217	0.7	164	7.5	232	9.75
	240	0.7	217	7.5	246	9.75
	240	22.7	217	23.5	246	24.5
	610	22.7	608	23.5	575	24.5
	610	37	608	30	575	35
SPFD	350	0	290	0	371	0
	350	3	290	2	371	4.8
	430	3	323	2	268	4.8
	430	15	323	7.1	268	16
	980	15	221	7.1	932	16
	980	36	221	15	932	35
			873	15		
		873	30			
SPRD	144	0	291	0	241	0
	144	0.6	291	6	241	2.1
	462	0.6	322	6	343	2.1
	462	6.3	322	11.5	343	4.5
	763	6.3	1015	11.5	384	4.5
	763	30	1015	35	384	9.1
					400	9.1
				400	13	
				1019	13	
				1019	30	
IP01	218	0	155	0	171	0
	218	1.5	155	4	171	3.9
	441	1.5	250	4	302	3.9
	441	12.5	250	6.6	302	10.75
	1180	12.5	347	6.6	1183	10.75
	1180	35	347	11.25	1183	30
			1130	11.25		
		1130	35			
IP02	146	0	247	0	213	0
	146	1.1	247	11	213	3
	301	1.1	461	11	313	3
	301	4.1	461	28.5	313	18.5
	349	4.1	1725	28.5	545	18.5
	349	34	1725	35	545	35.5
	1773	34			666	35.5
	1773	40			666	40
IP03	228	0	234	0	377	0
	228	6	234	7.6	377	7
	476	6	394	7.6	514	7
	476	27	394	24.8	514	22
	1200	27	1142	24.8	579	22
	1200	36	1142	35	579	41
					1102	41
					1102	50
IP04	278	0	271	0	278	0
	278	1.6	271	13.5	278	7.8
	379	1.6	833	13.5	458	7.8
	379	12.2	833	30.5	458	16.8
	606	12.2	1938	30.5	567	16.8
	606	33	1938	40	567	32.7
	1977	33			1660	32.7
	1977	35			1660	35
IP05	334	0	198	0	198	0
	334	23.6	198	5	198	5
	940	23.5	241	5	257	5
	940	30	241	10.2	257	10.2
			321	10.2	341	10.2
			321	18.5	341	19.1
			1096	18.5	980	19.1
			1096	35	980	35

(Continued)

Ground-motion site effects from multimethod shear-wave velocity characterization

APPENDIX.Vs VERSUS DEPTH PROFILES FOR THREE METHODS EMPLOYED AT EACH OF 16 PORTABLE SEISMOGRAPH STATIONS (*Continued*)

Site	SH body wave		ReMi		MASW	
	Vs (m/s)	Depth (m)	Vs (m/s)	Depth (m)	Vs (m/s)	Depth (m)
LD01	175	0	278	0	331	0
	175	1.2	278	8	331	5.25
	408	1.2	531	8	385	5.25
	408	5.6	531	21.25	385	14
	482	5.6	1999	21.25	466	14
	482	22.2	1999	30	466	22.25
	2060	22.2			1991	22.25
	2060	36			1991	30
LD05	163	0	290	0	315	0
	163	0.7	290	7.3	315	4.4
	250	0.7	387	7.3	354	4.4
	250	2.7	387	16.9	354	13.7
	403	2.7	580	16.9	580	13.7
	403	15.2	580	23.3	580	24
	748	15.2	1400	23.3	1039	24
	748	27.2	1400	35	1039	35
	1000	27.2				
	1000	30				
NP9985	329	0	246	0	277	0
	329	19	246	4.75	277	5.5
	707	19	317	4.75	374	5.5
	707	35	317	15.5	374	16.75
			399	15.5	500	16.75
			399	32	500	30
			894	32	752	30
			894	35	752	35
UoM1	279	0	327	0	208	0
	279	3.3	327	1.4	208	2.25
	880	3.3	403	1.4	398	2.25
	880	13	403	13	398	6.1
	1930	13	1899	13	551	6.1
	1930	30	1899	35	551	13.25
					1899	13.25
					1899	35
UoM2	250	0	200	0	243	0
	250	1.6	200	17.5	243	6.75
	415	1.6	312	17.5	259	6.75
	415	55	312	32	259	14.5
	1000	55	664	32	306	14.5
			664	35	306	35.4
					560	35.4
					560	40

Note: SH—horizontal shear wave; Vs—shear-wave velocity; ReMi—refraction microtremor; MASW—multichannel analysis of surface waves.

REFERENCES CITED

- Aki, K., 1988, Local site effects on strong ground motion, *in* Proceedings, Earthquake Engineering and Soil Dynamics II: Recent Advances in Ground-Motion Evaluation: Reston, Virginia, American Society of Civil Engineers, p. 103–155.
- Allen, T.I., and Wald, D.J., 2009, On the use of high-resolution topographic data as a proxy for seismic site conditions (VS30): *Seismological Society of America Bulletin*, v. 99, no. 2A, p. 935–943, doi:10.1785/0120080255.
- Asten, M.W., and Boore, D.M., 2005, Comparison of Shear-Velocity Profiles of Unconsolidated Sediments near the Coyote Borehole (CCOC) Measured with Fourteen Invasive and Non-Invasive Methods: U.S. Geological Survey Open-File Report 2005-1169, 35 p.
- Bailey, C.M., and Owens, R.E., 2012, Traversing suspect terraces in the center Virginia Piedmont: From Proterozoic anorthosites to modern earthquakes, *in* Eppes, M.C., and Bartholomew, M.J., eds., From the Blue Ridge to the Coastal Plain: Field Excursions in the Southeastern United States: Geological Society of America Field Guide 29, p. 327–344, doi:10.1130/2012.0029(10).
- Bard, P.Y., 1999, Microtremor measurements: A tool for site effect estimation?, *in* Irikura, K., Kudo, K., Okada, H., and Sasatani, T., eds., The Effect of Surface Geology on Seismic Motion: Rotterdam, Balkema, p. 1251–1279.
- Bingham, E., 1991, The physiographic provinces of Virginia: *Virginia Geographer*, v. 23, p. 19–32.
- Boore, D., 2004, Can site response be predicted?: *Journal of Earthquake Engineering*, v. 8, special issue, p. 1–41, doi:10.1080/13632460409350520.
- Boore, D.M., and Brown, L.T., 1998, Comparing shear-wave velocity profiles from inversion of surface-wave phase velocities with downhole measurement: Systematic differences between the CXW method and downhole measurement at six USC strong-motion sites: *Seismological Research Letters*, v. 69, p. 222–229, doi:10.1785/gssrl.69.3.222.
- Boore, D.M., Joyner, W.B., and Fumal, T.E., 1997, Equations for estimating horizontal response spectra acceleration from western North American earthquakes: A summary of recent work: *Seismological Research Letters*, v. 68, p. 128–153, doi:10.1785/gssrl.68.1.128.
- Borcherdt, R.D., 1970, Effects of local geology on ground motion near San Francisco Bay: *Seismological Society of America Bulletin*, v. 60, no. 1, p. 29–61.
- Borcherdt, R.D., 1994, Estimates of site-dependent response spectra for design (methodology and justification): *Earthquake Spectra*, v. 10, p. 617–653, doi:10.1193/1.1585791.
- Borcherdt, R.D., and Glassmoyer, G., 1992, On the characteristics of local geology and their influence on ground motions generated by the Loma Prieta earthquake in the San Francisco Bay region, California: *Seismological Society of America Bulletin*, v. 82, no. 2, p. 603–641.

- Building Seismic Safety Council, 2000, NEHRP (National Earthquake Hazards Reduction Program) Recommended Provisions for Seismic Regulations for New Buildings and Other Structures, Part I: Provisions: Washington, D.C., Federal Emergency Management Agency, FEMA 368, 392 p.
- Castellaro, S., Mulargia, F., and Rossi, P.L., 2008, *Vs30*: Proxy for seismic amplification?: *Seismological Research Letters*, v. 79, p. 540–543, doi:10.1785/gssrl.79.4.540.
- Chang, J., Herrmann, R.B., and Crossley, D.J., 2011, Joint inversion of surface-wave dispersion and first-arrival times for the determination of shallow P- and S-velocity structure [abs.]: *Seismological Research Letters*, v. 82, p. 328, doi:10.1785/gssrl.82.2.273.
- Chapman, M., 2013, On the rupture process of the 23 August 2011 Virginia earthquake: *Seismological Society of America Bulletin*, v. 103, no. 2A, p. 613–628, doi:10.1785/0120120229.
- Çoruh, C., Bollinger, G.A., and Costain, J.K., 1988, Seismogenic structures in the central Virginia seismic zone: *Geology*, v. 16, p. 748–750, doi:10.1130/0091-7613(1988)016<0748:SSITCV>2.3.CO;2.
- Cramer, C.H., Gombert, J.S., Schweig, E.S., Waldron, B.A., and Tucker, K., 2004, The Memphis, Shelby County, Tennessee, Seismic Hazard Maps: U.S. Geological Survey Open-File Report 2004-1294, 41 p.
- Crampton, S., and Lovell, J.H., 1991, A decade of shear-wave splitting in the Earth's crust: What does it mean? what use can we make of it? and what should we do next?: *Geophysical Journal International*, v. 107, p. 387–407, doi:10.1111/j.1365-246X.1991.tb01401.x.
- Dal Moro, G., and Papan, M., 2007, Joint inversion of surface wave dispersion curves and reflection travel times via multi-objective evolutionary algorithms: *Journal of Applied Geophysics*, v. 61, p. 56–81, doi:10.1016/j.jappgeo.2006.04.001.
- Dobry, R., Borcherdt, R.D., Crouse, C.B., Idriss, I.M., Joyner, W.B., Martin, G.R., Power, M.S., Rinne, E.E., and Seed, R.B., 2000, New site coefficients and site classification system used in recent building seismic code provisions: *Earthquake Spectra*, v. 16, p. 41–67, doi:10.1193/1.1586082.
- Foti, S., Parolai, S., Albarello, D., and Picozzi, M., 2011, Application of surface-wave methods for seismic site characterization: *Surveys in Geophysics*, v. 32, p. 777–825, doi:10.1007/s10712-011-9134-2.
- Frankel, A.D., Carver, D.L., and Williams, R.A., 2002, Nonlinear and linear site response and basin effects in Seattle for the M 6.8 Nisqually, Washington, earthquake: *Seismological Society of America Bulletin*, v. 92, p. 2090–2109, doi:10.1785/0120010254.
- Frankel, A.D., Stephenson, W.J., and Carver, D.L., 2009, Sedimentary basin effects in Seattle, Washington: Ground-motion observations and 3D simulations: *Seismological Society of America Bulletin*, v. 99, p. 1579–1611, doi:10.1785/0120080203.
- Harmsen, S.C., 1997, Determination of site amplification in the Los Angeles urban area from inversion of strong-motion records: *Seismological Society of America Bulletin*, v. 87, p. 866–887.
- Harris, J., 2005, Observation of shear-wave splitting in Quaternary sediments of the New Madrid Seismic Zone: An indicator of in-situ stress conditions?, in *Symposium on the Application of Geophysics to Engineering and Environmental Problems*: Atlanta, Georgia, Environmental and Engineering Geophysical Society, p. 952–958.
- Hatcher, R.D., Odom, A.L., Engelder, T., Dunn, D.E., Wise, D.U., Geiser, P.A., Schmael, S., and Kish, S.A., 1988, Characterization of Appalachian faults: *Geology*, v. 16, p. 178–181, doi:10.1130/0091-7613(1988)016<0178:COAF>2.3.CO;2.
- Horton, J.W., and Williams, R.A., 2012, The 2011 Virginia earthquake: What are scientists learning?: *Eos (Transactions, American Geophysical Union)*, v. 93, no. 33, p. 317–318, doi:10.1029/2012EO330001.
- Hough, S.E., 2012, Initial assessment of the intensity distribution of the 2011 Mw 5.8 Mineral, Virginia, earthquake: *Seismological Research Letters*, v. 83, p. 649–657, doi:10.1785/0220110140.
- Hughes, K.S., Hibbard, J.P., and Miller, B.V., 2013, Relationship between the Ellisville pluton and Chopawamsic fault: Establishment of significant late Ordovician faulting in the Appalachian piedmont of Virginia: *American Journal of Science*, v. 313, p. 584–612, doi:10.2475/06.2013.03.
- International Code Council, 2006, *The International Building Code*: Washington, D.C., International Code Council, 303 p.
- Ivanov, J., Miller, R.D., Xia, J., Steeples, D., and Park, C.B., 2006, Joint analysis of refractions with surface waves: An inverse solution to the refraction-traveltime problem: *Geophysics*, v. 71, no. 6, p. R131–R138, doi:10.1190/1.2360226.
- Jibson, R.W., and Harp, E.L., 2012, Landslide limits from 23 August 2011 Mineral, Virginia earthquake: *Seismological Society of America Bulletin*, v. 102, p. 2368–2377, doi:10.1785/0120120055.
- Joyner, W.B., Warrick, R.E., and Fumal, T.E., 1981, The effect of Quaternary alluvium on strong ground motion in the Coyote Lake, California, earthquake of 1979: *Seismological Society of America Bulletin*, v. 71, p. 1333–1349.
- Kendall, M.G., 1970, *Rank Correlation Methods*: London, Charles Griffin & Company Ltd., 160 p.
- Kramer, S.L., 1996, *Geotechnical Earthquake Engineering*: Upper Saddle River, New Jersey, Prentice-Hall, 653 p.
- Lampshire, L.D., Coruh, C., and Costain, J.K., 1994, Crustal structures and the eastern extent of lower Paleozoic shelf strata within the central Appalachians: A seismic reflection interpretation: *Geological Society of America Bulletin*, v. 106, p. 1–18, doi:10.1130/0016-7606(1994)106<0001:CSATEE>2.3.CO;2.
- Louie, J.N., 2001, Faster, better: Shear-wave velocity to 100 meters depth from refraction microtremor arrays: *Seismological Society of America Bulletin*, v. 91, p. 347–364, doi:10.1785/0120000098.
- McNamara, D.E., Benz, H., Herrmann, R., Bergman, E.A., Earle, P., Meltzer, A., Withers, M., and Chapman, M., 2014a, The Mw 5.8 central Virginia earthquake of August 2011 and aftershock sequence: Constraints on earthquake source parameters and fault geometry: *Seismological Society of America Bulletin*, v. 104, p. 40–54, doi:10.1785/0120130058.
- McNamara, D.E., Gee, L., Benz, H., and Chapman, M., 2014b, Frequency dependent seismic attenuation in the eastern US as observed from the 2011 central Virginia earthquake and aftershock sequence: *Seismological Society of America Bulletin*, v. 104, p. 55–72, doi:10.1785/0120130045.
- McNamara, D.E., Stephenson, W.J., Odum, J.K., Williams, R.A., and Gee, L., 2015, this volume, Site response in the eastern United States: A comparison of Vs30 measurements with estimates from horizontal:vertical spectral ratios, in Horton, J.W., Jr., Chapman, M.C., and Green, R.A., eds., *The 2011 Mineral, Virginia, Earthquake, and Its Significance for Seismic Hazards in Eastern North America*: Geological Society of America Special Paper 509, doi:10.1130/2015.2509(04).
- Molnar, S., Dosso, S.E., and Cassidy, J.F., 2010, Bayesian inversion of microtremor array dispersion data in southwestern British Columbia: *Geophysical Journal International*, v. 183, p. 923–940, doi:10.1111/j.1365-246X.2010.04761.x.
- Mooney, H.M., 1984, *Handbook of Geophysical Exploration, Volume 1: Seismic*: Minneapolis, Minnesota, Seismic Bison Instruments, 103 p.
- Moss, R.E.S., 2008, Quantifying measurement uncertainty of thirty-meter shear-wave velocity: *Seismological Society of America Bulletin*, v. 98, p. 1399–1411, doi:10.1785/0120070101.
- Mulargia, F., and Castellaro, S., 2008, Passive imaging in nondiffuse acoustic wavefields: *Physical Review Letters*, v. 100, p. 218,501–218,504, doi:10.1103/PhysRevLett.100.218501.
- Nogoshi, M., and Igarashi, T., 1971, On the amplitude characteristics of microtremor, Part II: *Seismological Society of Japan Journal*, v. 24, p. 26–40.
- O'Connell, D., and Turner, J.P., 2011, Interferometric multichannel analysis of surface waves (IMASW): *Seismological Society of America Bulletin*, v. 101, p. 2122–2141, doi:10.1785/0120100230.
- Odum, J.K., Stephenson, W.J., McNamara, D.E., and Williams, R.A., 2013, VS30 and spectral response from collocated shallow, active- and passive-source VS data at 27 sites in Puerto Rico: *Seismological Society of America Bulletin*, v. 103, p. 2709–2728, doi:10.1785/0120120349.
- Park, C.B., and Miller, R.D., 2008, Roadside passive multichannel analysis of surface waves (MASW): *Journal of Environmental & Engineering Geophysics*, v. 13, p. 1–11, doi:10.2113/JEEG13.1.1.
- Park, C.B., Miller, R.D., and Xia, J., 1999, Multichannel analysis of surface waves: *Geophysics*, v. 64, p. 800–808, doi:10.1190/1.1444590.
- Pratt, T.L., Coruh, C., and Costain, J.K., 1988, A geophysical study of the Earth's crust in central Virginia: Implications for Appalachian crustal structure: *Journal of Geophysical Research*, v. 93, no. B6, p. 6649–6667, doi:10.1029/JB093iB06p06649.
- Rosenblad, B.L., and Li, J., 2009, Comparative study of refraction microtremor (ReMi) and active source methods for developing low-frequency surface wave dispersion curves: *Journal of Environmental & Engineering Geophysics*, v. 14, p. 101–113, doi:10.2113/JEEG14.3.101.
- Socco, L.V., Foti, S., and Boiero, D., 2010, Surface-wave analysis for building near-surface velocity models—Established approaches and new perspectives: *Geophysics*, v. 75, no. 5, p. 75A83–75A102, doi:10.1190/1.3479491.

Ground-motion site effects from multimethod shear-wave velocity characterization

- Stephenson, W.J., Louie, J.N., Pullammanappallil, S., Williams, R.A., and Odum, J.K., 2005, Blind shear-wave velocity comparison of ReMi and MASW results with boreholes to 200 m in Santa Clara Valley: Implications for earthquake ground-motion assessment: *Seismological Society of America Bulletin*, v. 95, p. 2506–2516, doi:10.1785/0120040240.
- Strobbia, C., and Cassiani, G., 2011, Refraction microtremors: Data analysis and diagnostics of key hypotheses: *Geophysics*, v. 76, no. 3, p. MA11–MA20, doi:10.1190/1.3560246.
- Thompson, E.M., and Wald, D.J., 2012, Developing Vs30 site-condition maps by combining observations with geologic and topographic constraints, *in* Proceedings, 15th World Conference on Earthquake Engineering: Lisbon, Spain, Institute of Engineering Mechanics, 9 p.
- Thompson, E.M., Baise, L.G., Kayen, R.E., and Guzina, B.B., 2009, Impediments to predicting site response: Seismic property estimation and modeling simplifications: *Seismological Society of America Bulletin*, v. 99, p. 2927–2949, doi:10.1785/0120080224.
- Tinsley, J., Hough, S.E., Yong, A., Kanamori, H., Yu, E., Appel, V., and Wills, C., 2004, Geotechnical characterization of TriNet sites: *Seismological Research Letters*, v. 75, p. 505–514, doi:10.1785/gssrl.75.4.505.
- Wald, D.J., and Allen, T.I., 2007, Topographic slope as a proxy for seismic site conditions and amplification: *Seismological Society of America Bulletin*, v. 97, p. 1379–1395, doi:10.1785/0120060267.
- Wald, L.A., and Mori, J., 2000, Evaluation of methods for estimating linear site-response amplification in the Los Angeles region: *Seismological Society of America Bulletin*, v. 90, no. 6B, p. S32–S42, doi:10.1785/0119970170.
- Williams, R.A., Stephenson, W.J., Odum, J.K., and Worley, D.M., 2003, Comparison of P- and S-wave velocity profiles from surface seismic reflection refraction and downhole data: *Tectonophysics*, v. 368, p. 71–88, doi:10.1016/S0040-1951(03)00151-3.
- Wills, C.J., and Silva, W., 1998, Shear-wave velocity characteristics of geologic units in California: *Earthquake Spectra*, v. 14, p. 533–556, doi:10.1193/1.1586014.
- Wills, C.J., Petersen, M., Bryant, W.A., Reichle, M., Saucedo, G.J., Tan, S., Taylor, G., and Treiman, J., 2000, A site-conditions map for California based on geology and shear-wave velocity: *Seismological Society of America Bulletin*, v. 90, no. 6B, p. S187–S208, doi:10.1785/0120000503.
- Xia, J., Miller, R.D., Park, C.B., Hunter, J.A., Harris, J.B., and Ivanov, J., 2002, Comparing shear-wave velocity profiles inverted from multichannel surface waves with borehole measurements: *Soil Dynamics and Earthquake Engineering*, v. 22, p. 181–190, doi:10.1016/S0267-7261(02)00008-8.
- Yong, A., Hough, S.E., Iwahashi, J., and Braveman, A., 2012, A terrain-based site-conditions map of California with implications for the contiguous United States: *Seismological Society of America Bulletin*, v. 102, p. 114–128, doi:10.1785/0120100262.
- Zelt, C.A., and Smith, R.B., 1992, Seismic traveltime inversion for 2-D crustal velocity structure: *Geophysical Journal International*, v. 108, p. 16–34, doi:10.1111/j.1365-246X.1992.tb00836.x.
- Zhao, J.X., and Xu, H., 2013, A comparison of Vs30 and site period as site-effect parameters in response spectral ground-motion prediction equations: *Seismological Society of America Bulletin*, v. 103, p. 1–18, doi:10.1785/0120110251.
- Zywicki, D.J., 2007, The impact of seismic wave-field and source properties on ReMi estimates, *in* Nazarian, S., Yu, X., and Rosenblad, B.L., eds., Proceedings, Innovative Applications of Geophysics in Civil Engineering: Reston, Virginia, American Society of Civil Engineers, p. 1–10, doi:10.1061/40908(227)5.

MANUSCRIPT ACCEPTED BY THE SOCIETY 6 JUNE 2014

